A Simulation of Height Datum Transfer from the Mainland to an Island Using the Optical Clock Frequency Comparison Method

Hoang, A. T.,* **Dau, K. T., Tran, H. T., Pham, T. H. and Tran, D. D.**
School of Agriculture and Natural Resources, Vinh University, Vietnam
E-mail: anhthe.dhv@gmail.com,* ORCID ID: 0000-0002-6157-5436*
**Corresponding Author*

DOI: https://doi.org/10.52939/ijg.v21i12.4647

Abstract
Orthometric height (H) is an important geophysical parameter widely applied in scientific research, civil planning, and engineering projects. However, when oceans separate the two points or the measurement points are on islands, it is not easy to connect the heights between them using classical measurement methods (such as spirit levelling combined with gravimetry). This study aimed to simulate the transfer of height datum from the mainland to an island using the Optical Fiber Frequency Transfer (OFFT) method, based on the principles of relativistic geodesy. A simulation was performed with two points approximately 200 km apart: one on the mainland (Hanoi station) and one on an island (Bach Long Vi Station). The optical clock Ca^+ with a stability of 3.0×10^{-18} was placed at each point, and the two clocks were connected by an optical fiber. The main purpose of the simulation was to determine the geopotential difference, and consequently the orthometric height difference, between the stations from the measured relativistic frequency shift, providing an alternative to classical methods. The simulation utilized geopotential data and existing height control points as input data for the model setup. Besides, errors that affect the frequency difference measurement results have been added to the model. Through a numerical simulation, the obtained orthometric height for the Bach Long Vi island station was 13.968 m ± 0.022 m (its true height is 13.965 m). The simulation results presented in this study demonstrate the potential of the OFFT method for transmitting height datum from the mainland to an island or for connecting height systems between islands. However, real-world implementation faces practical challenges related to connecting the optical fibers and deploying ultra-stable optical clocks.

Keywords: Frequency Transfer, Height Datum Transfer, OFFT, Optical Fiber, Orthometric Height

1. Introduction

Height is one of the important geographical parameters in life, widely used in construction, traffic, scientific research, etc. Some of the activities requiring precise height have high societal impacts, such as: a) sea level rise [1], b) storm surges and coastal inundation [2], c) floods and evacuation route planning [3], d) crustal motion [4], and e) subsidence and other surface deformations due to seismic, mining, or other events [5]. To successfully monitor and manage such events regionally (e.g., floods) or globally (e.g., sea level rise), height information needs to be not only accurate but also refer to the same zero-height reference surface (vertical datum) [6] and [7]. Depending on the reference surface, there are several types of heights, such as orthometric height, normal height, dynamic height, and geodetic height. Each type of height has its advantages, and the method of determining it is also different. Among these types of heights, orthometric height is crucial and frequently used in practice due to its physical significance in engineering works [8].

There are many methods to determine the orthometric height of a point. The first method is to use a levelling instrument. The levelling method, combined with gravity data, yields high-accuracy results, at the centimeter to millimeter level [9]. Most countries use spirit levelling methods to establish height systems based on mean sea level. However, this method can accumulate significant errors when the two measurement points are far apart. The second method, the GNSS method, emerged in the 1900s and provides more rapid height data between distant points. However, the height that GNSS provides is ellipsoidal height, which is of limited use to surveyors and builders.

To obtain the orthometric height from GNSS results, geoid undulation must be determined. However, accurately determining this value is complex and typically requires the use of geoid models to provide an approximate value [10].

Recently, determining the height of points on islands has become very important. This involves the construction of structures on islands, marking a nation's sovereignty over the islands, etc. However, sea level cannot be used to transfer height from the mainland to the islands or to connect the height systems between islands. The ocean surface is not flat due to the influence of many factors, including waves, wind, tides, and gravity. Therefore, each country that uses mean sea level as the basis for its national height system will have different, non-uniform height systems. Currently, there are over 100 different local height systems around the world [11]. Scientists are constantly looking for new high-precision measuring methods to solve these difficulties, and applying relativistic geodesy is a promising method.

Relativistic geodesy is based on Einstein's general theory of relativity (GTR). According to GTR, there is a close relationship between clock frequency and gravity, called gravitational redshift. This means that a clock at a higher position will run faster than a clock at a lower position. Thus, when comparing the frequencies of clocks at two points, the geopotential difference between those two points can be determined. There are various methods to determine the gravity frequency shift between two points: transporting clocks between two stations [12][13][14] and [15]; connecting two stations by an optical fiber (optical fiber frequency transfer - OFFT) or a coaxial cable [16][17][18][19][20][21] and [22]; and transmitting frequency signals among different stations on the ground via GNSS satellites [23][24][25][26][27] and [28]. Among these methods, at present, the OFFT method offers the highest accuracy [20][21] and [22]. The advantage of transmitting light signals via optical fiber is that it can cancel out significant environmental noise, which would otherwise greatly influence measurement quality. An experiment using a pair of transportable clocks to determine the geopotential difference as well as the orthometric height difference between two points was conducted at Tokyo Skytree [29]. One clock was kept at the tower's base, and the other was transported to the observation deck 450 meters up. The two clocks were connected by an optical fiber. After about 6 months of measurements, the height difference measured by frequency shift was 452.596±0.013 m while by the GNSS method was 452.650±0.039 m, by laser ranging was 452.631±0.013 m. Another experiment was conducted using a portable Ca^+ optical clock with a systematic uncertainty of 1.3×10^{-17} [30]. First, the transportable clock was compared to the stationary laboratory clock. The two clocks were connected by an optical fiber with a length of 100 m at the same site. Then, the two clocks were separated with an orthometric height difference of 4.3 m. The result showed that the orthometric height difference calculated from the frequency shift according to general relativity was 4.22±0.33 m. This value was in consistent with the result 4.34±0.03 m measured by the conventional approach (spirit levelling).

This study is a simulation that applies the OFFT method to determine the height difference between two points separated by the ocean or sea. Based on this, an optical fiber clock network to connect height systems between islands is proposed in Section 2. The results of the simulation of the transfer of a height datum from Hanoi to Bach Long Vi island are presented in Section 3. Discussions are presented in Section 4 and the final section is Conclusion.

2. Method

2.1 Gravity Frequency Shift Method

The basic principle of the relativistic geodesy method is based on Einstein's GTR: the frequency of an electromagnetic wave changes during its propagation due to the effect of the gravity field, this change is called the gravity frequency shift [31].

The relativistic geodesy method uses the gravity frequency shift equation to determine the geopotential difference (as well as the orthometric height difference) between two points on the ground. Suppose a transmitting station located at point P emits frequency signal f_P. A station at point Q receives the frequency f_Q. According to GTR, the relationship between frequency shift and geopotential difference of the two points P and Q, expressed in Equation 1 [32][33] and [34]:

$$\frac{f_Q - f_P}{f} = -\frac{W_Q - W_P}{c^2}$$

Equation 1

Where f is the nominal frequency of the station clock, c is the speed of light in a vacuum, W_P and W_Q are the geopotentials at points P and Q. In this study, the definition of geopotential in physical geodesy is used, which means W is always non-negative ($W \geq 0$), unlike the definition in physics. Thus, if point P is above the geoid, then $W_P < W_0$ (W_0 is the geopotential of the points on the geoid). Equation 1 is the gravity frequency shift equation. From Equation 1, the geopotential difference ΔW_{PQ} can be determined using Equation 2 [20]:

$$\Delta W_{\mathrm{PQ}} = -\frac{\Delta f_{\mathrm{PQ}}}{f} c^2$$

Equation 2

Where $\Delta W_{\mathrm{PQ}} = W_{\mathrm{Q}} - W_{\mathrm{P}}$; $\Delta f_{\mathrm{PQ}} = f_{\mathrm{Q}} - f_{\mathrm{P}} = f' - f$. Equation 2 shows that, after the frequency shift Δf_{PQ} is measured, the geopotential difference ΔW_{PQ} can be determined. After obtaining the geopotential difference value, the orthometric height difference is determined as follows.

The orthometric height H_{P} of the point P on the Earth's surface is defined in Equation 3 [35]:

$$H_P = \frac{C_P}{\bar{g}_P}$$

Equation 3

Where $\bar{g}_{\mathrm{P}}$ is the mean value of the gravity along the plumb line between the geoid (P_0) and the surface point (P); C_P is the geopotential number.

Accurate determination of the value of $\bar{g}_P$ is a significant challenge because it requires complete knowledge of the crust's mass density. Therefore, an approximation is given to calculate this value using Equation 4 [35]:

$$\bar{g}_P = g_P - \left(\frac{1}{2}\frac{\partial \gamma}{\partial h} + 2\pi G_P\right) H_P$$

Equation 4

Where g_{P} is the observed gravity at each levelling station, G is Newton's gravitational constant, ρ is density of the Earth's crust, $\partial\gamma/\partial h$ is normal gravity gradient. By substituting nominal values: G = 66.7×10^{-9} $\mathrm{cm^3 g^{-1} sec^{-2}}$; ρ = 2.67 $\mathrm{g/cm^3}$; $\partial\gamma/\partial h$ = 0.3086 mGal/m, one obtains Equation 5 [35]:

$$\bar{g}_P = g_P + 0.0424 H_P$$

Equation 5

In this study, the impact of the approximation error on the results due to Equation 5 being an approximate equation is ignored. Substituting Equation 5 into Equation 3 yields the resulting height, which is often referred to as the Helmert orthometric height and used in practice for numerical computations of heights above the geoid, as shown in Equation 6 [35]:

$$H_P = \frac{C_P}{g_P + 0.0424 H_P}$$

Equation 6

Since Equation 6 has H_{P} on both sides, therefore it is usually solved through iteration.

Figure 1 shows the frequency comparison method. In this figure, the black dashed lines represent the equipotential surface passing through points P and Q, the black line is the geoid. P', Q'' are the intersection points of plumb lines passing through P, Q and the geoid; H_{P} and H_{Q} are the orthometric heights of points P and Q; W_{P}, W_{Q}, and W_0 are the geopotentials at points P, Q, and on the geoid; f_{P} is the frequency transmitted from the optical clock set at point P, f_{Q} is the frequency obtained by the optical detector set at point Q. Suppose at two points P and Q two optical clocks are placed, the frequency determined at each clock is f_{P} and f_{Q}, respectively. From Equation 6, one obtains Equation 7 [20]:

$$H_P = \frac{C_P}{g_P + 0.0424 H_P} = -\frac{W_P - W_0}{g_p + 0.0424 H_P}$$

Equation 7

Where g_{P} is surface gravity measurement at point P, in $\mathrm{m/s^2}$, and W in $\mathrm{m^2/s^2}$.

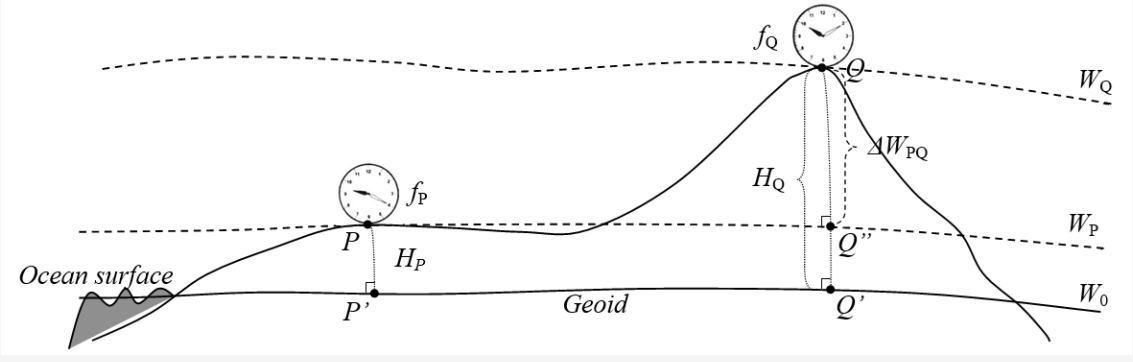

Figure 1: Determination of the orthometric height difference by comparing clock frequencies [20]

Suppose the height of point P is known, and one needs to determine the height of point Q. Combining Equation 2 and Equation 7, the orthometric height of the point Q can be determined using Equation 8 [20]:

$$H_Q = -\frac{W_P - W_0}{g_Q + 0.0424H_Q} + \frac{c^2}{g_Q + 0.0424H_Q}\frac{\Delta f_{PQ}}{f}$$

Equation 8

Where g_Q is surface gravity measurement at point Q, the frequency shift Δf_{PQ} is determined by the gravity frequency shift method.

Therefore, according to Equation 7 and Equation 8, one obtains Equation 9 [20]:

$$H_Q = \frac{H_P(g_P + 0.0424H_P)}{g_Q + 0.0424H_Q} + \frac{c^2}{g_Q + 0.0424H_Q}\frac{\Delta f_{PQ}}{f}$$

Equation 9

From Equation 9, if H_P is known, and measure the frequency shift value Δf_{PQ}, then H_Q can be determined.

With the development of optical fiber manufacturing technology [36][37] and [38] and the accuracy of the optical clock [39] and [40], currently, the optical fiber frequency transfer technique is the best accuracy method in frequency shift determining methods [21][22][26] and [41].

2.2 Connecting Height Systems Between Islands

The OFFT method has many advantages in determining height differences, such as high accuracy, the frequency signal is not affected by environmental errors, and no limitation due to the distance between stations. However, when stations are far apart, the frequency transmission process will suffer from attenuation. If the distance is greater than the guaranteed length, there must be reasonable signal compensation through the use of amplifiers [16] and [42]. In a study in Germany, nine EDFAs (Erbium-doped fiber amplifiers) were used along a 920 km fiber link connecting Max-Planck-Institut für Quantenoptik (MPQ) in Garching, Germany, and Physikalisch-Technische Bundesanstalt (PTB) in Braunschweig, Germany [16]. Another study used broad-band amplifiers and bidirectional amplifiers for a 1400 km of fiber optic cable connecting LNE-SYRTE in Paris, France and PTB in Braunschweig, Germany [42].

How is the OFFT method used to connect the height system between the islands? Suppose on the mainland there are S_A and S_B stations that already have height and stations S_1, S_2, S_3, ..., S_n are on the islands (Figure 2).

Figure 2: Schematics connecting height systems between islands

In Figure 2, stations S_A and S_B (yellow squares) are located on the mainland, separated by the ocean; S_i (blue squares) are located on islands, connected by optical fibers (red dashed line). The height of these S_i stations needs to be determined. Suppose station S_A emits a signal with frequency f_A, and S_1 receives this frequency, then the frequency shift between S_A and S_1 can be determined as $\Delta f_{A1} = f_1 - f_A$. Station S_1 emits a signal with frequency f_1, station S_2 receives this frequency, and the frequency shift between S_1 and S_2 is determined as $\Delta f_{12} = f_2 - f_1$. Finally, station S_n emits a signal with frequency f_n, station S_B receives this frequency, and the frequency shift between S_n and S_B is determined as $\Delta f_{nB} = f_B - f_n$.

From the Δf_i values, the height difference between the stations (Δh_{A1}, Δh_{12}, Δh_{23}, ..., Δh_{nB}) can be determined. Starting from the height of station S_A is H_A, the heights of other stations can be determined based on the obtained height differences. At station S_B, the height H_B is determined using Equation 10:

$$H_B = H_A + \Delta h_{A1} + \Delta h_{12} + \ldots + \Delta h_{(n-1)n} + \Delta h_{nB} \quad \text{Equation 10}$$

Applying the principle of weighted error distribution as with the classical method (This means that measurements with smaller errors will have larger weights), the heights of station S_B can be determined after the adjustment of the stations.

3. Simulation Transfer of Height Datum from Hanoi to Bach Long Vi Island

In this study, a simulation is established using two optical clocks connected by an optical fiber link to transfer height from Hanoi to Bach Long Vi island. In this simulation, an optical clock station is placed at each point (Hanoi and Bach Long Vi island) and connect them by an optical fiber. These stations have a known H value. Simulated observations are generated, and from there, the simulated H values are calculated. This value is then compared with the true H value to determine the differences of method. The geopotential values of the stations are determined by the EGM2008 model, which then calculates the frequency shift values. Random errors are added to these values to obtain new frequency shift values, which are called observed values. From this observed value, use the H value of Hanoi station as a datum, recalculating the new H value of Bach Long Vi station. The difference between these two H values of the Bach Long Vi station is the accuracy of height transmission using the OFFT method. The scheme of the simulator is in Figure 3. Suppose the two stations *A* and *B* are connected by optical fiber. The frequency f_{AB} is transmitted from station *A* to station *B*, the errors are added to create observation value f'_{AB}, obtained at station *B*. Similarly, the frequency f_{BA} is transmitted from station *B* to station *A*, resulting in the observation value f'_{BA} at station *A*. By combining f'_{AB} and f'_{BA}, the simulated gravity frequency shift value is obtained, from which the simulated geopotential difference between the two stations and the simulated H value of station *B* are calculated. The accuracy of the OFFT method is evaluated by comparing the simulated H value to the true H value.

3.1 Input Data of the Simulation

To transfer the height datum from Hanoi to Bach Long Vi island (Figure 4), two datum stations are used: Lang station in Hanoi (is a height reference station in Vietnam's height system) and BLV station in Bach Long Vi island (is a national CORS station of Vietnam). In Figure 4, the yellow points are optical clock station and red curve is optical fiber.

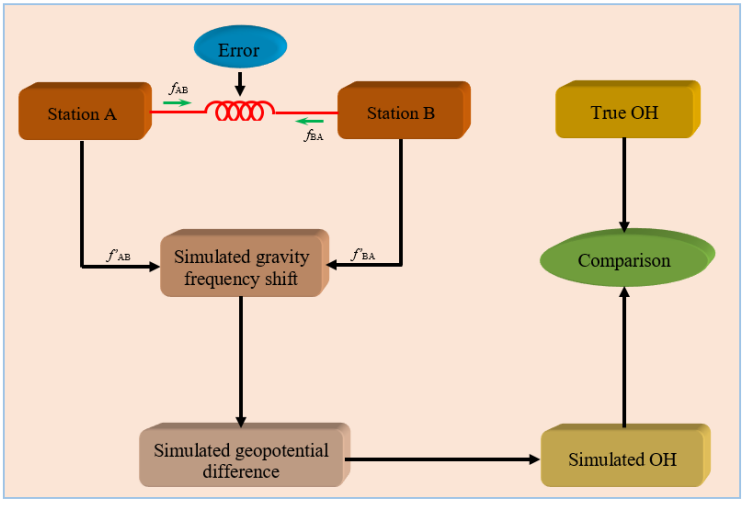

Figure 3: The scheme of the simulator

From the coordinates of the two stations, the EGM2008 model [43] is used to determine the geopotential values W; the gravity values g; and the geoid undulation N values at the stations. The orthometric height of the stations will be calculated according to the formula: $H = h - N$, in which, h is taken from information of the national CORS stations. These values are considered true values (These values are the best available geodetic value derived from the EGM2008 model). The optical clock used in the simulation is a Ca^+ optical clock [44] with a stability of 3.0×10^{-18}. This is a liquid nitrogen-cooled optical clock to reduce the temperature of the blackbody radiation (BBR) shield in the vacuum chamber. The liquid nitrogen tank, which is approximately 0.8 m high and 5 mm thick, is constructed from oxygen-free copper, offering good thermal conductivity. The hyper-Ramsey method and a high-order servo algorithm are employed to reduce the uncertainty caused by the laser light shift of the probe and the servo error. More details of the optical clock are presented in [44]. One assumes that the two stations use the same type of clock and have the same stability. To connect two clocks, single-mode fiber is used to limit dispersion errors. The distance of about 200km between the two stations is not too long, so intermediate stations and EDFAs are not needed. Information about the clock stations and related parameters of the simulation is listed in Table 1. A total of 720 observation values has been generated for this study.

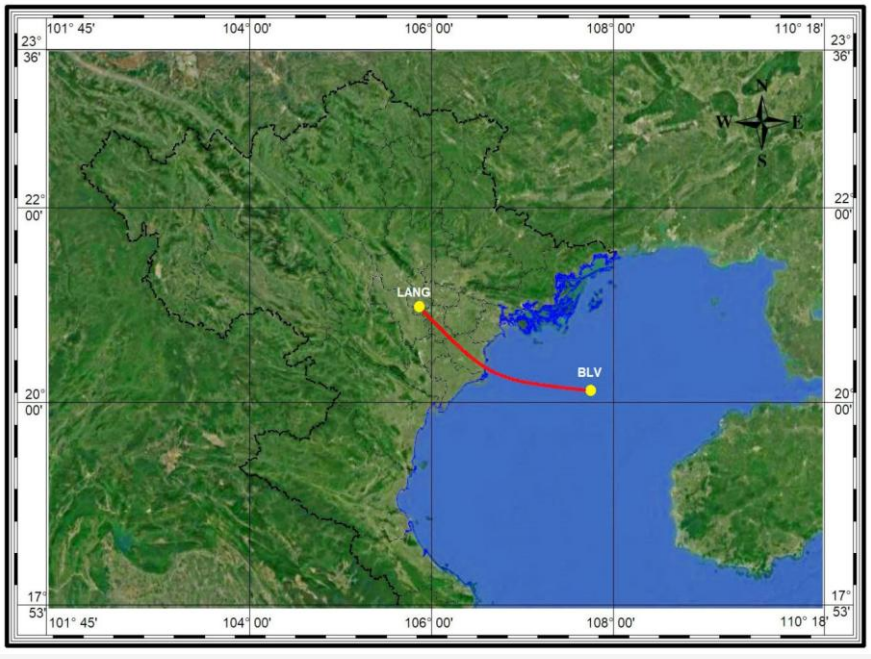

Figure 4: Height datum transfer from Hanoi (Lang station) to Bach Long Vi island (BLV station) use comparing optical clock frequency signals via OFFT technique

Table 1: Relevant parameters used in optical clock network simulation

Station	Abbreviation	Values of Parameters
LANG (Hanoi)	Coordinate	21.025121^0N, 105.804781^0E
	H	27.435 m
	W	6.2636583E+07 $m^2.s^{-2}$
	g	9.7864383 $m.s^{-2}$
BLV (Bach Long Vi)	Coordinate	20.12917^0N, 107.72266^0E
	H	13.965 m
	W	6.2636715E+07 $m^2.s^{-2}$
	g	9.7862585 $m.s^{-2}$
Optical clock Ca^+	stability	3.0×10^{-18}
Number of observed values		720

3.2 Simulation Data Processing

From Equation 2, based on the geopotential values W of two stations (LANG and BLV), the frequency shift value can be calculated using Equation 11 [20]:

$$\Delta f_{LANG-BLV} = -\frac{W_{BLV} - W_{LANG}}{c^2} f$$

Equation 11

Where $\Delta f_{(LANG\ -\ BLV)obs}$ is the simulated observation value. To obtain the values of $\Delta f_{(LANG\ -\ BLV)obs}$, the errors are added to the $\Delta f_{(LANG\ -\ BLV)}$ value calculated from Equation 11. In this simulation, the error sources of the OFFT method are considered [20]: clock errors δ_{clock}, dispersion errors δ_{Dis}, Doppler error δ_{Dop}, fiber nonlinearities errors δ_{Non}, equipment delay errors δ_{delay} and fiber itself errors δ_{fib}. Determining the magnitude of these errors plays an important role in generating observed values, making the simulation closer to reality. The total errors δ_{total} is calculated using Equation 12 [22]:

$$\delta_{total} = \delta_{clock} + \delta_{Dis} + \delta_{Dop} + \delta_{Non} + \delta_{delay} + \delta_{fib}$$

Equation 12

In this simulation, the Ca^+ optical clock as introduced in [44], with a stability of 3×10^{-18}, is used. This is considered one of the most precise clocks available today. Therefore, the clock error is set to 3×10^{-18}. The Doppler error δ_{Dop} can be removed by using the Doppler noise cancellation technique [41]. Therefore, in this simulation, the Doppler error δ_{Dop} is assumed to be canceled. Similarly, the fiber itself errors δ_{fib} will be eliminated if the two-way frequency transmission technique is used. Since the two-way frequency transmission technique is employed here, the fiber itself error δ_{fib} is excluded. The remaining errors were presented in [45]. With the use of single-mode fiber in the simulation, most of the effect of dispersion error has been eliminated. The remaining highly influential component is polarization dispersion error. The magnitude of polarization dispersion error is determined to be about 8×10^{-18} [45]. The nonlinear error was determined to be about 1×10^{-19} with a clock laser stability of 1×10^{-16} [44]. Delay error is controlled below 1×10^{-18}. Details of the errors are listed in Table 2.

After determining the magnitude of the error sources, these errors are treated as noises and are added to the true value to make the observed values. A random noise generation method with white Gaussian noise is used to make observed values. The observed values were generated using a random noise model implemented in MATLAB. The total observation period for this simulation was set to 30 days, with data collected at one-hour intervals. Consequently, 720 observation values were obtained. The final result obtained is the series of two-way observed values, as shown in Figure 5. The blue line illustrates the frequency data variation, revealing that the simulation data is relatively stable, with no sudden fluctuations. The average value of the two observed directions was the frequency shift value between two stations. From the observed frequency shift value, the observed geopotential difference ($\Delta W_{(\text{LANG-BLV})\text{obs}}$) can be calculated according to Equation 2. Next, from the orthometric height of LANG station (H_{LANG}), the orthometric height of Bach Long Vi station ($H_{(\text{BLV})\text{obs}}$) can be calculated according to the Equation 9.

Compare $H_{(\text{BLV})\text{obs}}$ and H_{BLV}, the difference between these two values can be calculated using Equation 13 [22]:

$$\delta H = H_{(BLV)} - H_{(BLV)obs}$$

Equation 13

3.3 Simulation Results

From the observed values, Equations (2) and (9) were used to calculate 720 orthometric height values for Bach Long Vi station, as presented in Figure 6. In Figure 6, the blue points represent the observed orthometric height values for Bach Long Vi station, while the red line indicates the true orthometric height value for this station.

Table 2: Error magnitudes of different error sources in simulate OFFT method

Error sources	Error magnitudes
Optical clock	~ 3×10^{-18} [44]
Polarization dispersion	~ 8×10^{-18} [45]
Delay effect	~ 1×10^{-18} [20]
Nonlinear effects	~ 1×10^{-19} [44]
Doppler effect	Removed by using the Doppler noise cancellation technique [41]
Fiber itself effect	Removed by using use two-way frequency transmission technique [41]
Total	1.21×10^{-17}

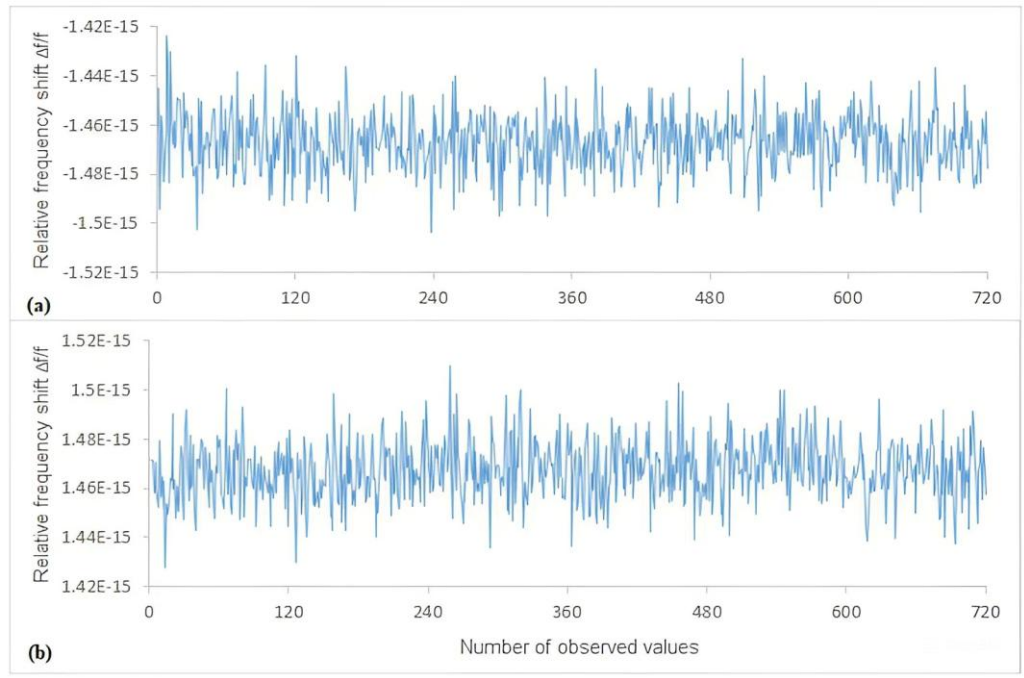

Figure 5: The two-way observed values. Figure 5a is the frequency transmission from the LANG station to the BLV station, and Figure 5b is the opposite, the frequency transmission from the BLV station to the LANG station

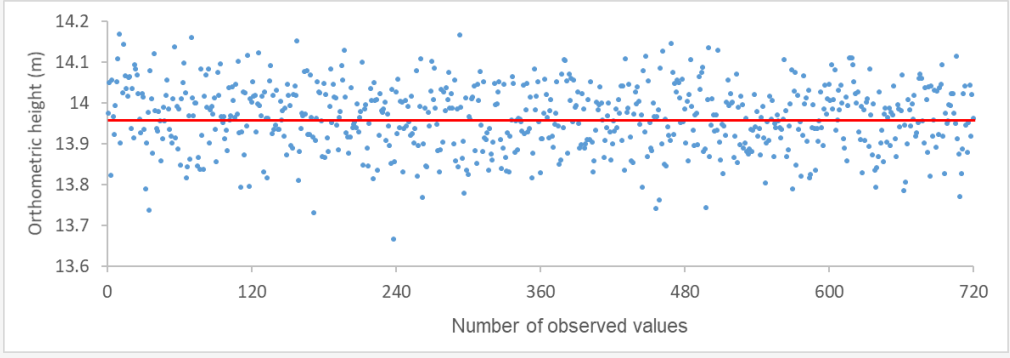

Figure 6: The 720 orthometric height values of the BLV station

To increase the accuracy and generality, the simulation was performed 10 times, with each time generating 720 observation values using different random noise. The final result is determined by calculating the weighted mean and the standard error of the mean for measurements with varying standard deviations. The final results are shown in Table 3 and Figure 7.

The data in Table 3 show that the change in the H value, as well as its STD, is minimal, remaining only at the centimeter level. This level of accuracy is sufficient to meet the requirements for establishing National levelling network (Fourth-Order) [46]. The difference in the H values across the 10 observations is due to random noise generated by the simulation. The values of the standard deviations demonstrate consistency with the assumptions regarding the model's input errors (in Table 2). If these errors were better controlled in practice (e.g., by using higher-precision clocks, improved frequency transmission, etc.), the overall accuracy of the results would be significantly enhanced. From Table 3, the difference between the two orthometric height values $H_{(\mathrm{BLV})\mathrm{obs}}$ and H_{BLV} can be calculated. The results are shown in Table 4. From Table 4, it can be seen that the difference between the orthometric height determined by the OFFT method and the true orthometric height of Bach Long Vi station is at the centimeter level. Figure 7 demonstrates that the error in the observations is largely uniform.

Table 3: Results of 10 observations

Observed No.	Observed orthometric height (m)	STD (m)
1	13.969	0.056
2	13.967	0.053
3	13.964	0.053
4	13.968	0.080
5	13.961	0.080
6	13.964	0.083
7	13.965	0.073
8	13.976	0.077
9	13.974	0.062
10	13.970	0.070
Average	13.968	0.022

Table 4: Difference between the two orthometric height values

Station	True orthometric height (m)	Observed orthometric height (m)	Difference between the two values (m)
BLV	13.965	13.968 ± 0.022	0.003

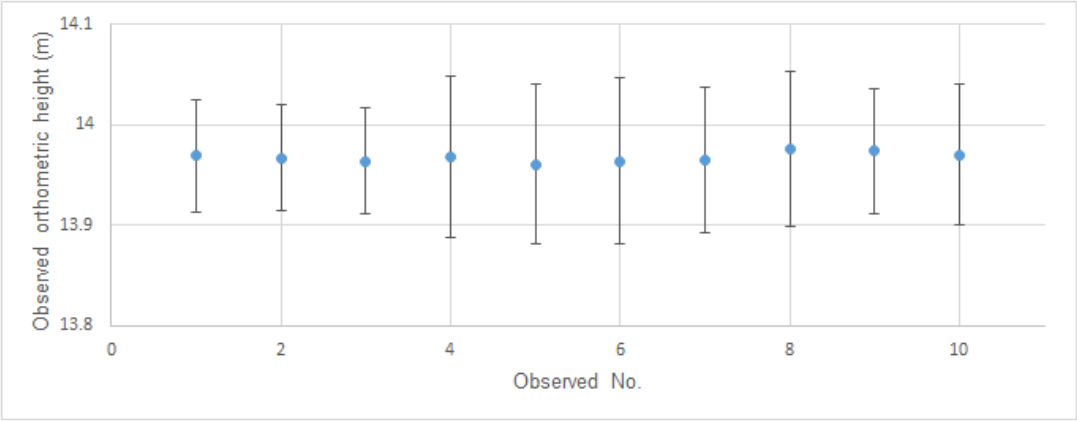

Figure 7: The orthometric height values of the BLV station and its STD values in 10 time observations

The results of this simulation once again prove that the OFFT method can determine the height difference with an accuracy at the centimeter. With this accuracy, it can be confirmed that the OFFT method is currently the method with the highest accuracy among the gravity frequency shift approaches.

4. Discussions

Currently, optical clocks are the highest-precision clocks (the stability at 10^{-19} to 10^{-18} level). According to relativistic geodesy, this accuracy guarantees the determination of orthometric height at the centimetre level. Moreover, this method allows the determination of geopotential differences and thus enables the determination of height differences in any reference system. This capability is an important application for connecting height systems across oceans where classical methods are infeasible. In this simulation, utilizing two optical clocks with a stability of 3×10^{-18} over a 200 km distance, the orthometric height determination yielded a standard error of the mean of ± 0.022 m across 10 simulation runs. The resulting uncertainty of ±2.2 cm, over the 200 km distance, is acceptable for national establishment levelling network standards (second-order) [46]. For individual measurements, the accuracy ranges from 5.6 cm to 8.3 cm, which meets the requirements for establishing a fourth-order national levelling network [46]. This confirms the potential feasibility of the OFFT method for critical national geodetic infrastructure.

The results of this simulation align closely with real-world experimental results, such as those in Tokyo, Japan [29] (achieving ± 0.013 m), demonstrating that our model accurately reflects state-of-the-art clock performance. Furthermore, this accuracy significantly surpasses the results obtained by the GNSS-based time-frequency transfer, which yielded deviations up to 0.59 m [47]. In addition, this result also shows that the OFFT method has higher accuracy than the GPS levelling method (achieving ±0.169 m [48] and ±0.286 m [49]), which has been widely studied and used. It is important to note that simulation errors are controlled, unlike the complex error sources encountered in real-world conditions. Nevertheless, the simulation results demonstrate the potential of the OFFT method for determining orthometric height with centimeter-level accuracy, if the technical challenges are effectively managed.

The most significant constraint of the OFFT method is the requirement for a dedicated, high-stability fiber-optic connection, which involves substantial implementation and maintenance costs, particularly for submarine installations. Fortunately, single-mode cables are commonly used for data transmission in today's information transmission work due to their ability to transmit data over distances of hundreds of kilometers with low optical loss. However, it is crucial to note that most existing telecommunication fibers are not built to the phase noise and stability specifications (10^{-18}) required for relativistic frequency transfer. Overcoming these technical challenges requires complex and expensive upgrades (e.g., bi-directional stabilization systems, Erbium-doped fiber amplifiers) to the cables currently used to transmit information data. To overcome this limitation, alternative solutions such as clock comparison by frequency propagation in free space [50][51] and [52] and the development of optical clocks that can operate stably outside the laboratory [53] are promising areas of research to overcome the infrastructure limitations.

5. Conclusions

Simulation results demonstrate that the OFFT method is a promising technique for determining the orthometric height difference between points separated by the ocean. With an optical clock with a stability of 3×10^{-18}, the standard deviation of the orthometric height difference result between two points 200 km apart is ± 2.2 cm. This precision makes OFFT the ideal tool for transferring national height datums from the mainland to islands and for unifying regional height systems. The findings support the full applicability of optical clocks for geodetic measurements. However, this method also faces many difficulties when deployed in practice, such as the requirements for clock stability, the need for a dedicated fiber optic connection between measuring points, and the technical challenge of high-stability frequency transmission. The large initial investment, the high stability requirements of the clock, and the technical challenges in ensuring the stability of the frequency transmission process in optical fibers over long distances are still the main practical barriers to large-scale OFFT method application.

Therefore, the next step should address the technical and economic feasibility of implementing this technology. Specifically, future research should focus on solving the technical and cost issues associated with upgrading existing submarine fiber optic infrastructure or deploying stable dedicated fiber optic lines for a pilot national OFFT network. In parallel, research into the fabrication of highly stable and compact optical clocks is also an important task in the effort for the practical deployment of the OFFT method.

References

[1] Din, A. H. M., Zulkifli, N. A., Hamden, M. H. and Aris, W. A. W., (2019). Sea Level Trend Over Malaysian Seas from Multi-Mission Satellite Altimetry and Vertical Land Motion Corrected Tidal Data. *Advances in Space Research*, Vol. 63(11); 3452-3472. https://doi.org/10.1016/j.asr.2019.02.022.

[2] Nguyen, J. and Kuleshov, Y., (2023). Coastal Inundation Hazard Assessment in Australian Tropical Cyclone Prone Regions. *Hydrology*, Vol. 10(12). https://doi.org/10.3390/hydrology10120228.

[3] Van de Sande, B., Lansen, J. and Hoyng, C., (2012). Sensitivity of Coastal Flood Risk Assessments to Digital Elevation Models. *Water*, Vol. 4(3), 568-579. https://doi.org/10.3390/w4030568.

[4] Yokota, Y., Ishikawa, T. and Watanabe, Si., (2018). Seafloor Crustal Deformation Data along the Subduction Zones Around Japan Obtained by GNSS-A Observations. *Scientific Data*, Vol. 5. https://doi.org/10.1038/sdata.2018.182.

[5] Kersten, T., Kobe, M., Gabriel, G., Timmen, L., Schön, S. and Vogel, D., (2017). Geodetic Monitoring of Subrosion-Induced Subsidence Processes in Urban Areas: Concept and Status Report. *Journal of Applied Geodesy*, Vol. 11(1); 21-29. https://doi.org/10.1515/jag-2016-0029.

[6] Gruber, T., Agren, J., Angermann, D., Ellmann, A., Engfeldt, A., Gisinger, C., Jaworski, L., Marila, S., Nastula, J., Nilfouroushan, F., Oikonomidou, X., Poutanen, M., Saari, T., Schlaak, M., Świątek, A., Varbla, S. and Zdunek, R., (2020). Geodetic SAR for Height System Unification and Sea Level Research-Observation Concept and Preliminary Results in the Baltic Sea. *Remote Sensing*, Vol. 12(22). https://doi.org/10.3390/rs12223747.

[7] Arif, M. I., Din, A. H. M., Zulkifli, N. A., Hamden, M. H., Omar, A. H. and Adzmi, N. H. M., (2023). Assessment of Sea Level Rise Impact on Peninsular Malaysia Geodetic Vertical Datum. *The International Archives of the Photogrammetry, Remote Sensing and Spatial Information Sciences*, Vol. XLVIII-4/W6-2022; 25–32. https://doi.org/10.5194/isprs-archives-XLVIII-4-W6-2022-25-2023.

[8] Vaníček, P. and Santos, M., (2019). What Height System Should be Used in Geomatics? *International Journal of Earth & Environmental Sciences*, Vol. 4. https://doi.org/10.15344/2456-351X/2019/160.

[9] Allister, N. A. and Featherstone, W. E., (2001). Estimation of Helmert Orthometric Heights Using Digital Barcode Levelling, Observed Gravity and Topographic Mass-Density Data Over Part of the Darling Scarp, Western Australia. *Geomatics Research Australasia*, Vol. 75, 25-52.

[10] Barzaghi, R., De Gaetani, C. I. and Betti, B., (2020). The Worldwide Physical Height Datum Project. *Rendiconti Lincei. Scienze Fisiche e Naturali*, Vol. 31(Suppl 1); 27–34. https://doi.org/10.1007/s12210-020-00948-0.

[11] Sideris, M. G., (2015). *Geodetic World Height System Unification.* Handbook Geomathematics, W. Freeden, Z. M. Nashed, and T. Sonar, Eds. Berlin, Germany, Springer, 3067-3085.

[12] Mai, E., (2013). *Time, Atomic Clocks, and Relativistic Geodesy*. Deutsche Geodätische Kommission, Reihe A, Theoretische Geodäsie, Heft Nr. 124, Verlag der Bayerischen Akademie der Wissenschaften: München, Germany.

[13] Grotti, J., Koller, S., Vogt, S., Häfner, S., Sterr, U., Lisdat, C., Denker, H., Voigt, C., Timmen, L., Rolland, A., Baynes, F., Margolis, H.S., Zampaolo, M., Thoumany, P., Pizzocaro, M., Rauf, B., Bregolin, F., Tampellini, A., Barbieri, P., Zucco, M., Costanzo, G.A., Clivati, C., Levi, F. and Calonico, D., (2018). Geodesy and Metrology with a Transportable Optical Clock. *Nature Physics*, Vol. 14; 437-441. https://doi.org/10.1038/s41567-017-0042-3.

[14] Liu, D., Cao, J., Yuan, J., Cui, K., Yuan, Y., Zhang, P., Chao, S., Shu, H. and Huang, X., (2023). Laboratory Demonstration of Geopotential Measurement Using Transportable Optical Clocks, *Chinese Physics B*, Vol. 32. https://doi.org/10.1088/1674-1056/ac6337.

[15] Grotti, J., Nosske, I., Koller, S. B., Herbers, S., Denker, H., Timmen, L., Vishnyakova, G., Grosche, G., Waterholter, T., Kuhl, A., Koke, S., Benkler, E., Giunta, M., Maisenbacher, L., Matveev, A., Dörscher, S., Schwarz, R., Al-Masoudi, A., Hänsch, T. W., Udem, Th., Holzwarth, R. and Lisdat, C., (2024). Long-Distance Chronometric Levelling with a Portable Optical Clock. *Physical Review Applied*, Vol. 21. https://doi.org/10.1103/PhysRevApplied.21.L061001.

[16] Predehl, K., Grosche, G., Raupach, S. M. F., Droste, S., Terra, O., Alnis, J., Legero, T., Hänsch, T. W., Udem, T., Holzwarth, R. and Schnatz, H., (2012). A 920-Kilometer Optical Fiber Link for Frequency Metrology at the 19th Decimal Place. *Science*, Vol. 336, 441-444. https://doi.org/10.1126/science.1218442.

[17] Shen, Z. Y. and Shen, W. B., (2015). Geopotential Difference Determination Using Optic-Atomic Clocks via Coaxial Cable Time Transfer Technique and a Synthetic Test. *Geodesy and Geodynamics*, Vol. 6 (5), 344–350. https://doi.org/10.1016/j.geog.2015.05.012.

[18] Takano, T., Takamoto, M., Ushijima, I., Ohmae, N., Akatsuka, T., Yamaguchi, A., Kuroishi, Y., Munekane, H., Miyahara, B. and Katori, H., (2016). Geopotential Measurements with Synchronously Linked Optical Lattice Clocks. *Nature Photonics*, Vol. 10; 662–666. https://doi.org/10.1038/nphoton.2016.159.

[19] Shen, Z. Y., Shen, W. B., Peng, Zh., Liu, T., Zhang, S. G. and Chao, D. B., (2019). Formulation of Determining the Gravity Potential Difference Using Ultra-High Precise Clocks via Optical Fiber Frequency Transfer Technique. *Journal of Earth Science*, Vol. 30; 422–428. https://doi.org/10.1007/s12583-018-0834-0.

[20] Hoang, A. T., Shen, Z. Y., Shen, W. B., Cai, C. H., Xu, W., Ning, A. and Wu, Y. F., (2021). Determination of the Orthometric Height Difference Based on Optical Fiber Frequency Transfer Technique. *Geodesy and Geodynamics*, Vol. 12; 405–412. https://doi.org/10.1016/j.geog.2021.08.003.

[21] Hoang, A. T., Shen, Z. Y., Wu, K., Ning, A. and Shen, W. B., (2022). Test of Determining Geopotential Difference between Two Sites at Wuhan Based on Optical Clocks' Frequency Comparisons. *Remote Sensing*, Vol. 14(19). https://doi.org/10.3390/rs14194850.

[22] Hoang, A. T., Shen, Z. Y. and Shen, W. B., (2023). Unifying the Regional Height System Using Optic-Fiber Clock Network: A Simulation Test for Southeast Asia. *IEEE Access*, Vol. 11, 92996-93003. https://doi.org/10.1109/ACCESS.2023.3308519.

[23] Delva, P., Hees, A., Bertone, S., Richard, E. and Wolf, P., (2015). Test of the Gravitational Redshift with Stable Clocks in Eccentric Orbits: Application to Galileo Satellites 5 and 6. *Classical and Quantum Gravity*, Vol. 32. https://doi.org/10.1088/0264-9381/32/23/232003.

[24] Shen, Z. Y., Shen, W. B. and Zhang, S. X., (2016). Formulation of Geopotential Difference Determination Using Optical-Atomic Clocks Onboard Satellites and on Ground Based on Doppler Cancellation System. *Geophysical Journal International*, Vol. 206; 1162–1168. https://doi.org/10.1093/gji/ggw198.

[25] Shen, Z. Y., Shen, W. B. and Zhang, S. X., (2017). Determination of Gravitational Potential at Ground Using Optical-Atomic Clocks on Board Satellites and on Ground Stations and Relevant Simulation Experiments. *Surveys in Geophysics*, Vol. 38, 757–780. https://doi.org/10.1007/s10712-017-9414-6.

[26] Shen, W. B., Sun, X., Cai, C. H., Wu, K. C. and Shen, Z. Y., (2019). Geopotential Determination Based on a Direct Clock Comparison Using Two-Way Satellite Time and Frequency Transfer. *Terrestrial, Atmospheric and Oceanic Sciences*, Vol. 30; 21–31. https://doi.org/10.3319/TAO.2018.07.09.02.

[27] Cai, C. H., Shen, W. B., Shen, Z. Y. and Xu, W., (2020). Geopotential Determination Based on Precise Point Positioning Time Comparison: A Case Study Using Simulated Observation. *IEEE Access*, Vol. 8; 204283–204294. https://doi.org/10.1109/ACCESS.2020.3036988.

[28] Xu, W., Shen, W. B., Cai, C. H., Li, L. H., Wang, L. and Shen, Z. Y., (2021). Modelling and Performance Evaluation of Precise Positioning and Time-Frequency Transfer with Galileo Five-Frequency Observations. *Remote Sensing*, Vol. 13. https://doi.org/10.3390/rs13152972.

[29] Takamoto, M., Ushijima, I., Ohmae, N., Yahagi, T., Kokado, K., Shinkai, H. and Katori, H., (2020). Test of General Relativity by a Pair of Transportable Optical Lattice Clocks. *Nature Photonics*, Vol. 14; 411–415. https://doi.org/10.1038/s41566-020-0619-8.

[30] Huang, Y., Zhang, H. Q., Zhang, B. L., Hao, Y. M., Guan, H., Zeng, M. Y., Chen, Q. F., Lin, Y. G., Wang, Y. Z., Cao, S. Y., Liang. K., Fang, F., Fang, Z. J., Li, T. C. and Gao, K. L., (2020). Geopotential Measurement with a Robust, Transportable Ca^{+} Optical Clock. *Physical Review A*, Vol. 102. https://doi.org/10.1103/PhysRevA.102.050802.

[31] Einstein, A., (1915). *The Field Equations of Gravitation*. Proceedings of the Royal Prussian Academy of Sciences, 48, 844–847.

[32] Bjerhammar, A., (1985). On a Relativistic Geodesy. *Bullentin Geodesique*, Vol. 59, 207-220. https://doi.org/10.1007/BF02520327.

[33] Shen, W. B., (1998). *Relativistic Physical Geodesy*. Habilitation. Graz Technical University, Graz.

[34] Shen, W. B., Ning, J. S., Liu, J. N., Li, J. C. and Chao, D. B., (2011). Determination of the Geopotential and Orthometric Height Based on Frequency Shift Equation. *Natural Science*, Vol. 3(5); 388-396. https://doi.org/10.4236/ns.2011.35052.

[35] Hofmann-Wellenhof, H. and Moritz, H., (2006). *Physical Geodesy*. Springer, Vienna. https://doi.org/10.1007/978-3-211-33545-1.

[36] Broadway, C., Min, R., Leal-Junior, A. G., Marques, C. and Caucheteur, C., (2019). Toward Commercial Polymer Fiber Bragg Grating Sensors: Review and Applications. *Journal of Lightwave Technology*, Vol. 37(11), 2605-2615. https://doi.org/10.1109/JLT.2018.2885957.

[37] Wang, H., Jiang, L. H. and Xiang P., (2018). Improving the Durability of the Optical Fiber Sensor Based on Strain Transfer Analysis. *Optical Fiber Technology*, Vol. 42(1), 97-104. https://doi.org/10.1016/j.yofte.2018.02.004.

[38] Wang, H., Xiang, P. and Jiang, L., (2019). Strain Transfer Theory of Industrialized Optical Fiber-Based Sensors in Civil Engineering: A Review on Measurement Accuracy, Design and Calibration. *Sensors and Actuators A: Physical*, Vol. 285, 414-426. https://doi.org/10.1016/j.sna.2018.11.019.

[39] Zhang, Z. Q., Kyle, J. A., Rattakorn, K. and Barett, D. B., (2023). Lu^+ Clock Comparison at the 10^{-18} Level via Correlation Spectroscopy. *Science Advances*, Vol. 9. https://doi.org/10.1126/sciadv.adg1971.

[40] Aeppli, A., Kim, K., Warfield, W., Safronova, M. S. and Ye, J., (2024). Clock with 8×10^{-19} Systematic Uncertainty. *Physical Review Letters*, Vol. 133. https://doi.org/10.1103/PhysRevLett.133.023401.

[41] Calonico, D., Bertacco, E. K., Calosso, C. E., Clivati, C., Costanzo, G. A., Frittelli, M., Godone, A., Mura, A., Poli, N., Sutyrin, D. V., Tino, G., Zucco, M. E. and Levi, F., (2014). High-Accuracy Coherent Optical Frequency Transfer over a Doubled 642-km Fiber Link. *Applied Physics B,* Vol. 117(3); 979-986. https://doi.org/10.1007/s00340-014-5917-8.

[42] Lisdat, C., Grosche, G., Quintin, N., Shi, C., Raupach, S. M. F., Grebing, C., Nicolodi, D., Stefani, F., Al-Masoudi, A., Dörscher, S., Häfner, S., Robyr, J.-L., Chiodo, N., Bilicki, S., Bookjans, E., Koczwara, A., Koke, S., Kuhl, A., Wiotte, F., Meynadier, F., Camisard, E., Abgrall, M., Lours, M., Legero, T., Schnatz, H., Sterr, U., Denker, H., Chardonnet, C., Le Coq, Y., Santarelli, G., Amy-Klein, A., Le Targat, R., Lodewyck, J., Lopez, O. and Pottie, P.-E., (2016). A Clock Network for Geodesy and Fundamental Science. *Nature Communications.*, Vol. 7; 12443. https://doi.org/10.1038/ncomms12443.

[43] Pavlis, N. K., Holmes, S. A., Kenyon, S. C. and Factor, J., (2012). The Development and Evaluation of the Earth Gravitational Model 2008 (EGM2008). *Journal of Geophysical Research: Solid Earth*, Vol. 117. https://doi.org/10.1029/2011JB008916.

[44] Huang, Y., Zhang, B. L., Zeng, M. Y., Hao, Y. M., Zang, H. Q., Guan, H., Chen, Z., Wang, M. and Gao, K. L., (2022). Liquid-Nitrogen-Cooled Ca^+ Optical Clock with Systematic Uncertainty of 3×10^{-18}. *Physical Review Applied*, Vol. 17. https://doi.org/10.1103/PhysRevApplied.17.034041.

[45] Williams, P. A., Swann, W. C. and Newbury, N. R., (2008). High-Stability Transfer of an Optical Frequency over Long Fiber-Optic Links, *Journal of the Optical Society of America B*, Vol. 25(8); 1284-1293. https://doi.org/10.1364/JOSAB.25.001284.

[46] Ministry of Natural Resources and Environment, 11/2008/QD-BTNMT, *National Technical Regulation on Height Network Establishment (Vietnamese).*

[47] Wu, K. C., Shen, W. B., Fok, H. S., Lian, Z. Z., Zhang, P. F., Li, L. H., Wang, L., Ning, A., Xu, R. and Shen, Z. Y., (2025). Measuring Intercontinental-Scale Geopotential Difference Using Atomic Clock Frequency Comparison with PPP Technique. *Advances in Space Research*. https://doi.org/10.1016/j.asr.2025.10.010.

[48] Raufu, I. O. and Tata, H., (2022). Comparison of Two Corrector Surface Models of Orthometric Heights from GPS/Levelling Observations and Global Gravity Model. *Journal of Geospatial Information Science and Engineering*, Vol. 5(1), 15-20. https://doi.org/10.22146/jgise.72531.

[49] Pratomo, D. G., Khomsin, K. and Khariz, S., (2018). Comparison of Sea Surface Variation Derived from Global Navigation Satellite System (GNSS) and Co-tidal in Java Sea. *E3S Web of Conferences: International Symposium on Global Navigation Satellite System 2018 (ISGNSS 2018)*. Vol. 94. Surabaya, Indonesia.

[50] Dix-Matthews, B. P., Schediwy, S. W., Gozzard, D. R., Savalle, E., Esnault, F.-X., Lévèque, T., Gravestock, C., D'Mello, D., Karpathakis, S. F., Tobar, M. E. and Wolf, P., (2021). Point-to-Point Stabilized Optical Frequency Transfer with Active Optics. *Nature Communications*, Vol. 12. https://doi.org/10.1038/s41467-020-20591-5.

[51] Bodine, M. I., Deschênes, J. D., Khader, I. H., Swann, W. C., Leopardi, H., Beloy, K., Bothwell, T., Brewer, S. M., Bromley, S, L., Chen, J-S., Diddams, S. A., Fasano, R. J., Fortier, T. M., Hassan, Y. S., Hume, D. B., Kedar, D., Kennedy, C. J., Koepke, A., Leibrandt, D. R., Ludlow, A. D., McGrew, W. F., Milner, W. R., Nicolodi, D., Oelker, E., Parker, T. E., Robinson, J. M., Romish, S., Schäffer, S. A., Sherman, J. A., Sonderhouse, L., Yao, J., Ye, J., Zhang, X., Newbury, N. R., Sinclair, L. C., (2020). Optical Atomic Clock Comparison Through Turbulent Air. *Physical Review Research*, Vol. 2. https://doi.org/10.1103/PhysRevResearch.2.033395.

[52] Shen, Q., Guan, J. Y., Zeng, T., Lu, Q. M., Huang, L., Cao, Y., Chen, J. P., Tao, T. Q., Wu, J, C., Hou, L., Liao, S, K., Ren, J. G., Yin, J., Jia, J. J., Jiang, H. F., Peng, C. Z., Zhang, Q. and Pan, J. W., (2021). Experimental Simulation of Time and Frequency Transfer via an Optical Satellite–Ground Link at 10^{-18} Instability. *Optica*, Vol. 8(4); 471-476. https://doi.org/10.1364/OPTICA.413114.

[53] Loh, W., Reens, D., Kharas, D., Sumant, A., Belanger, C., Maxson, R. T., Medeiros, A., Setzer, W., Gray, D., DeBry, K., Bruzewicz, C. D., Plant, J., Liddell, J., West, G. N., Doshi, S., Roychowdhury, M., Kim, M. E., Braje, D., Juodawlkis, P. W., Chiaverini, J. and McConnell, R., (2025). Optical Atomic Clock Interrogation Using an Integrated Spiral Cavity Laser. *Nature Photonics*, Vol. 19, 277–283. https://doi.org/10.1038/s41566-024-01588-8.